Molecular Crystals and Liquid Crystals
Publication details, including instructions for authors and subscription information:
http://www.tandfonline.com/loi/gmcl16

Effects of Molecular Length on Nematic Mixtures

J. David Margerum [a], John E. Jensen [a] & Anna M. Lackner [a]

[a] Hughes Research Laboratories, 3011 Malibu Canyon Road, Malibu, California, 90265, U.S.A.

Version of record first published: 14 Oct 2011.

To cite this article: J. David Margerum , John E. Jensen & Anna M. Lackner (1981): Effects of Molecular Length on Nematic Mixtures, Molecular Crystals and Liquid Crystals, 68:1, 137-156

To link to this article: http://dx.doi.org/10.1080/00268948108073560

Mol. Cryst. Liq. Cryst., 1981, Vol. 68, pp. 137–156
0026-8941/81/6801-0137 $06.50/0

Printed in the United States of America

Effects of Molecular Length on Nematic Mixtures

I. Anisotropic and Dynamic Scattering Properties of 4-Alkoxyphenyl 4-Alkylbenzoate Mixtures†

J. DAVID MARGERUM, JOHN E. JENSEN and ANNA M. LACKNER

Hughes Research Laboratories, 3011 Malibu Canyon Road, Malibu, California 90265, U.S.A.

(*Received August 11, 1980*)

The properties of nematic mixtures of 4-alkoxyphenyl 4-alkylbenzoates are studied as a function of their average molecular length ($\bar{L}$). The $\bar{L}$'s of the mixtures vary between 20.46 and 27.14 Å, but they all have clearpoints in the 51 to 58° C range. The flow viscosity increases linearly with $\bar{L}$. The dielectric constant, refractive index, birefringence, and density decrease linearly with $\bar{L}$, and the dielectric anisotropy becomes more negative. With tetrabutylammonium tetraphenylboride added as a salt dopant, the conductivity anisotropy ($\sigma_{\parallel}/\sigma_{\perp}$) decreases with increasing $\bar{L}$, and the dynamic-scattering (DS) threshold voltage increases correspondingly. The effect of $\bar{L}$ on the DS decay time (τ_D) is highly dependent on the surface alignment. In surface-$\perp$ cells, τ_D increases strongly with $\bar{L}$, while in surface-$\parallel$ cells, τ_D decreases slightly with increasing $\bar{L}$. The temperature dependence of $\sigma_{\parallel}/\sigma_{\perp}$ indicates that the longer $\bar{L}$ mixtures, with about ten or more total alkyl carbons from both end groups, have cybotactic nematic characteristics.

INTRODUCTION

Multicomponent liquid crystal (LC) mixtures are often used to widen the temperature range of nematics used in electrooptical device applications. Although there is an increasing amount of information being published on the properties of nematic mixtures of positive dielectric anisotropy for use in polarization switching displays, there is much less information on the properties of nematic mixtures of negative dielectric anisotropy for use in dynamic scatter-

† This paper is included in the proceedings of the Eighth International Liquid Crystal Conference since it is needed to supplement material in the companion paper which follows.

ing (DS) displays.[1,2] We are particularly interested in the use of *para*-substituted phenyl benzoate mixtures as relatively stable nematics for both dc- and ac-activated DS devices.[3-6] Therefore, we have begun a series of studies to investigate systematically the relationships between the structure of ester LC components and the properties of their mixtures. The present study is designed specifically to examine the effect of the average molecular length of 4-alkoxyphenyl 4-alkylbenzoate mixtures on their viscosity, conductivity anisotropy, dielectric anisotropy, DS threshold voltage, and DS response time.

EXPERIMENTAL

The phenyl benzoate components of the LC mixtures are prepared by reacting the appropriate *p*-alkoxyphenols and *p*-alkylbenzoyl chlorides. Whenever possible, the reactants are obtained commercially (Eastman or Aldrich). The esters are purified by several recrystallizations and are checked for purity by thin-layer chromatography and by liquid chromatography (Waters Assoc. Model ALC-202/401, with a microporasil column). We estimate by these methods that the impurity content is less than 0.5% in all of the esters and is less than 0.1% in most of them. In all cases, the materials have virtually no ionic impurities, and the resistivities of the undoped mixtures are greater than $10^{11}\Omega$-cm at room temperature. The heat of fusion (ΔH_f), melting point (mp), and clearpoint (clpt) are obtained by differential scanning calorimetry (DSC) using a Mettler TA2000B thermal analysis system. The transition temperatures correspond to the lower part of any range obtained from the DSC slope extrapolated back to the baseline. A computer program is used to calculate the mole fraction of selected components for eutectic mixtures by applying the Schroeder Van Laar equation.[7,8]

The flow viscosity is measured in calibrated (20 to 100 cS range) Cannon-Ubbelohde-type viscometer tubes (1.03-mm capillary bore size) held in a temperature-controlled water bath. Density measurements are made in calibrated pycnometer tubes. The refractive index and birefringence are measured with a Leitz-Jelly micro-refractometer. The dielectric anisotropy and conductivity anisotropy are measured using a previously described apparatus,[5] modified by installation of a thermally controlled copper block in the cavity to achieve better temperature control over a wider range. This required a larger magnetic pole spacing than used previously, which resulted in a 7-kG magnetic field. An LC thickness of 229 or 503 μm is used. Samples are doped with tetrabutylammonium tetraphenylboride (TBATPB) by adding 0.1% of this salt, warming to dissolve, and then filtering the LC through a 0.2-μm filter after letting it cool overnight. The DS threshold measurements are taken in transmission with unpolarized green light and an acceptance angle of $\pm 0.5°$ at the detector of the optical system.[5] The cells are made with 3.2-mm-thick glass

plates, with the LC contained by a 25.4-μm-thick polyester film perimeter spacer. These cells have indium tin oxide (ITO) conductive glass surfaces overcoated with SiO deposited at a 30° angle to produce surface-|| alignment of the LCs. The threshold voltages are obtained by extrapolating the initial steep decrease in transmission back to the baseline, using frequencies of 30 Hz. The decay times are taken from 10% to 90% T after activation at 30 V. To improve the reproducibility of decay times, measurements are made using thicker (12.7 mm) optical flats with an SiO_2-overcoated ITO surface and deposited pads of SiO_x in the corners as spacers. One set of these flats is ion-beam etched at a shallow angle for surface-|| alignment,[9] while a second set is spin-coated with an aqueous polyvinyl alcohol solution, baked in an oven, and rubbed gently for surface-|| alignment. The spacer thickness of the first cell is 15.86 μm and of the second is 15.43 μm. These cells are filled with doped LC, and the DS decay times are measured in a thermostated box. A third set of optical flats with a 15.90-μm spacing is used for surface-$\perp$ alignment by first bonding a long chain alcohol (n-$C_{18}H_{37}OH$) on the SiO_2 coating.[10] The LCs align perpendicular to the surface in this cell with very small off-normal tilt angles ($<0.5°$). Undoped LCs are used in this third cell for measurements of the Fréedericks transition threshold voltage at 1 kHz, while doped LCs are used for DS decay time studies after activation with voltages at 30 Hz.

The k_{11} elastic constants are determined from capacitance versus voltage curves on LC cells using an apparatus similar to that described by Meyerhofer.[11] The cells are made using ITO-coated glass plates (3.2 mm thick) with a 25.4-μm-thick polyester film perimeter spacer arranged to give an active area of 6.45 cm^2. The ITO is overcoated with 2000 Å of SiO_2, and surface-$\perp$ alignment is obtained by treatment with n-$C_{22}H_{45}OH$. The tilt angles are less than 0.5°. The measuring signal is 25 mV at 10 kHz, and the alignment bias control is variable up to 30 V_{rms} at 75 or 450 Hz. An empty cell is used to correct for the capacitance of the non-active area. The electronic components include a PAR Model 124A as a signal source and a lock-in amplifier, a Kiethley 427 current amplifier, and a Krohn-Hite 3322 variable filter (to help filter out the bias frequency).

RESULTS AND DISCUSSION

LC components and mixtures

The thermal properties of the phenyl benzoate compounds used in these mixtures are shown in Table I, where R and R′ are n-alkyl groups as shown by the general structure in Figure 1a. The melting points and heats of fusion from Table I are used to calculate the eutectic mixtures shown in Table II. None of the components are known to have any smectic phases. In addition to the letter designations (A, B, etc.) used for the mixtures in this paper, the specific

TABLE I
Thermal properties of components

Component			mp, °C		Clpt., °C		ΔH_f,
RO	R′	Code	Obs.	Lit.	Obs.	Lit.	kcal/mole
CH_3O	CH_3	10-1	96.2	97[a]	(10)[b]	—	7.20
C_2H_5O	C_3H_7	20-3	75.7	75.5[c]	68	68.5[c]	6.72
C_2H_5O	C_5H_{11}	20-5	62.8	62.1[c]	63	63.4[c]	7.49
C_4H_9O	CH_3	40-1	72.9	—	53	—	7.81
C_4H_9O	C_3H_7	40-3	70.7	71.3[c]	61	59.0[c]	8.15
C_4H_9O	C_6H_{13}	40-6	40.0	39[d]	49	49[d]	8.42
$C_6H_{13}O$	C_3H_7	60-3	51.8	51.6[c]	57.4	58.5[c]	5.52
$C_6H_{13}O$	C_4H_9	60-4	29	30.2[c]	48	48.4[c]	4.20
$C_6H_{13}O$	C_5H_{11}	60-5	40.9	40[e]	59.3	59[e]	5.77
$C_8H_{17}O$	C_3H_7	80-3	51.8	51.0[c]	56.8	59.1[c]	6.12
$C_8H_{17}O$	C_6H_{13}	80-6	44.9	46[f]	55.6	57[f]	8.12

[a] T. I. Gnilomedova *et al., Zh. Prikladnoi Khimmii,* **49,** 1337 (1976).
[b] Virtual nematic clpt.
[c] M. E. Neubert *et al., Liq. Cryst. and Ordered Fluids,* (Plenum Press, New York, 1974), **2,** p. 293, J. F. Johnson and R. S. Porter, Eds.
[d] R. Steinstrasser, *Z. Naturforsch.* **27b,** 774 (1972).
[e] J. P. Van Meter and B. H. Klanderman, *Mol. Cryst. Liq. Cryst.,* **22,** 271 (1973).
[f] GDR Patent 86269.

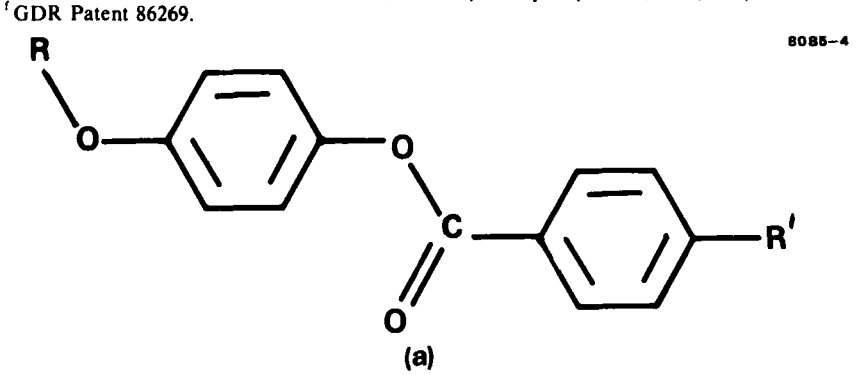

FIGURE 1 (a) General structure of LC mixture components. (b) Model of 4-hexyloxyphenyl 4-butylbenzoate (60-4) showing the molecular length (L = 25.78 Å) used.

TABLE II
Composition of liquid-crystal mixtures

Compound		Mole Fraction in Mixtures				
Code[a]	Length, Å	A	B	D	E	F
10-1	16.20	0.112	0.073	—	—	—
20-3	19.67	0.222	0.148	—	—	—
20-5	22.21	0.283	0.180	0.240	—	—
40-1	19.61	0.191	0.119	—	—	—
40-3	21.78	0.192	0.117	0.160	0.120	—
40-6	25.81	—	0.364	—	0.375	—
60-3	24.44	—	—	—	—	0.249
60-4	25.78	—	—	0.601	—	—
60-5	27.03	—	—	—	0.504	0.331
80-3	26.84	—	—	—	—	0.213
80-6	30.85	—	—	—	—	0.207
HRL Mixture Numbers		2N42	2N43	2N44	2N46	2N48

[a] See Table I.

Hughes identifications (HRL-2N42, etc.) are also shown. The latter are cited in other publications.[12,13] The molecular length (L) of each compound is measured from the end-to-end distance in CPK models, as indicated in Figure 1b. A fully extended configuration is used, with a twist angle of about 30° between the aromatic planes as described by Neubert *et al.*[14] Table III shows the average molecular length ($\bar{L}$) of the mixtures, and both the calculated and the observed nematic ranges. Several features are worth noting regarding the composition of these different length eutectic mixtures. For one thing, the compound 10-1 is used as a pseudo-nematic component even though it has not been observed to be an LC. Also, contrary to the guideline of making eutectic mixtures in which each component differs by more than 20% in overall molecular length,[8] we mix some components of the same, or nearly the same,

TABLE III
Average length and nematic range of RO-R′ mixtures[a]

Mixture	Average Length ($\bar{L}$), Å	Average Number of R+ R′ Carbons	mp, °C		Clpt., °C	
			Calc.	Obs.	Calc.	Obs.
A	20.39	5.61	28.8	5.3	57.0	57.7
B	22.37	7.21	18.2	−5.8	54.4	52.4
C[b]	23.36	8.20	—	2.4	57.2	55.6
D	24.31	8.82	24.9	−7.8	54.0	51.4
E	25.92	10.12	18.8	16.1	54.6	55.0
F	27.14	11.50	6.1	18.0	57.4	56.3

[a] Calculated as eutectic compositions, except Mixture C, with $\bar{L}$ calc. from mole fractions of components of various L's.
[b] Equal weight percent of A and F.

length. This is done when the R and R′ end groups of one component are substantially different from those of another component (e.g., 20–3 with 40–1, 20–5 with 40–3, 40–6 with 60–5, and 60–5 with 80–3).

No systematic variation is made in the components with regard to the odd/even number of end group carbons, nor to the end of the molecule on which the longest alkyl groups are used. (However, longer alkyl groups and longer length components are not used in order to avoid smectic components.) Although the properties of the mixtures are probably affected by such end group effects in addition to being affected by the average length, we believe that the general trends of the $\bar{L}$ effects that we report below are nevertheless valid.

Refractive indices, density, and dielectric constant

The refractive index and birefringence of the mixtures decrease linearly with increasing molecular length, as shown in Figure 2. The effect of the increasing length is to decrease the molecular polarizability of the molecules as the alkyl end groups are lengthened and dilute the polarizability effect due to the rest

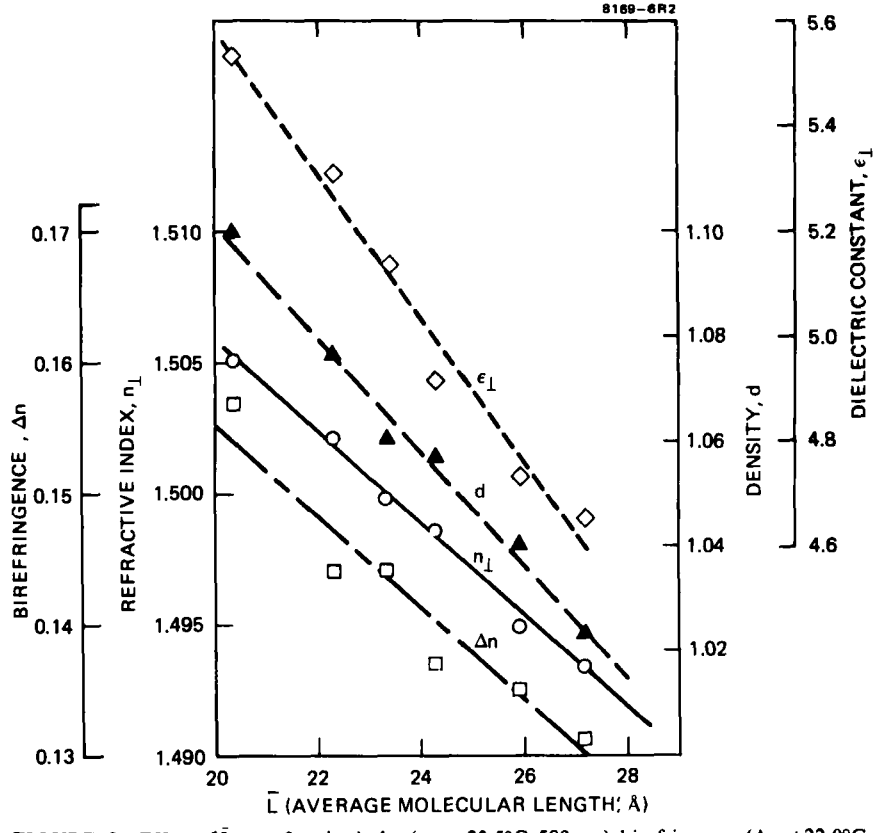

FIGURE 2 Effect of $\bar{L}$ on refractive index ($n_\perp$ at 23.5°C, 589 nm), birefringence (Δn at 22.0°C, 589 nm), density (d at 25.0°C), and dielectric constant ($\epsilon_\perp$ at 25.0°C).

of the molecule. The density of the mixtures also decreases with increasing average molecular length due to the increasing percentage of alkyl groups as compared with the aromatic ester group. A similar trend is also shown in Figure 2 for the dielectric constant ($\epsilon_\perp$) variation with $\bar{L}$, as longer alkyl groups dilute the effects of the more polar groups in the molecules. In these mixtures, the value of $\epsilon_\perp$ at 25°C decreases by about 0.15 units per added methylene group.

Viscosity

The flow viscosity (η) of the ester mixtures is studied as a function of temperature between 20 and 50° C. These flow viscosities should correspond approximately to the viscosity along the LC director,[15] corresponding to the Helfrich viscosity η_2 (or the Miesowicz viscosity η_B). Each mixture has as a linear relationship between log η and T^{-1} (in $°K^{-1}$), as shown in Figure 3. These viscosi-

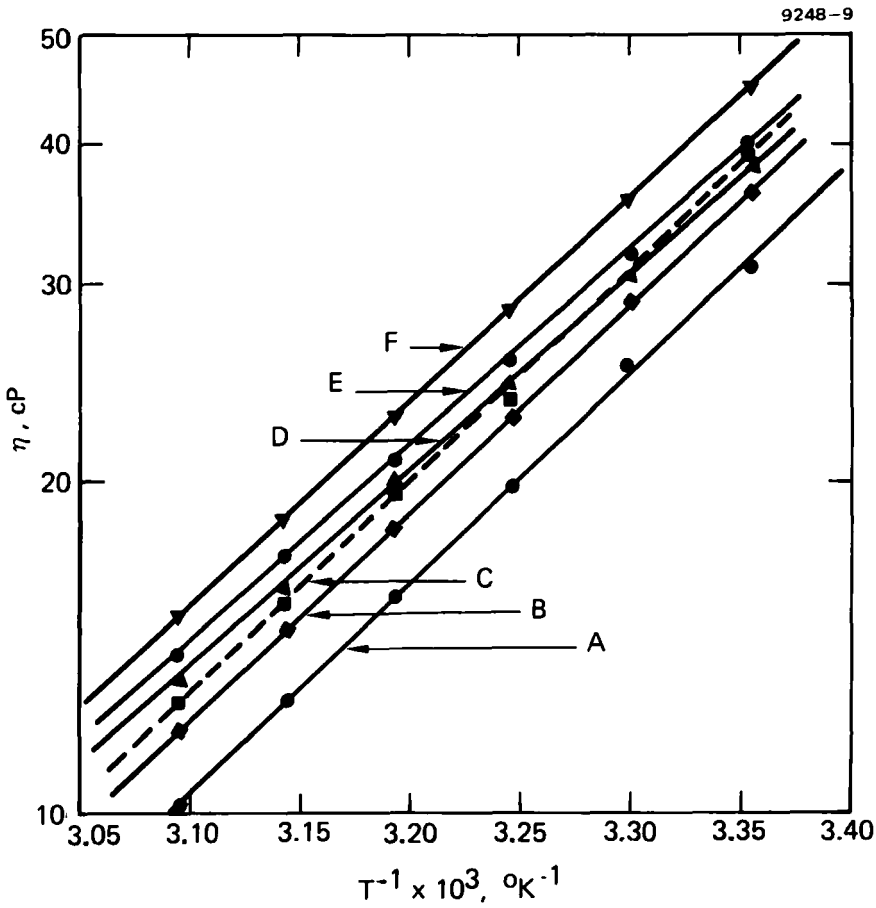

FIGURE 3 Viscosity of RO–R′ ester LC mixtures as a function of temperature.

ties are the same with or without the addition of the TBATPB salt dopant. The viscosities at 25 and 45° C are plotted against the average molecular length in Figure 4. The viscosity increases linearly with the average length, and the viscosity changes substantially over the range of lengths studied. The clearpoints of all the mixtures are within a range of about 6° C, and there is no obvious effect of their clearpoint differences on the viscosities. The results at 25° C in Figure 4 correspond to about a 1.8 cP increase in viscosity per each additional methylene group in the average molecular length of these ester mixtures. At 45° C, the increase in viscosity is about 0.9 cP per added methylene group.

Conductivity anisotropy

The conductivity anisotropy ($\sigma_{\parallel}/\sigma_{\perp}$) of TBATPB in each ester mixture is shown as a function of temperature in Figure 5. We found that at room temperature the $\sigma_{\parallel}/\sigma_{\perp}$ values of TBATPB in mixture A are constant with variations in the resistivity of the sample, and we have previously observed this same type of consistency of $\sigma_{\parallel}/\sigma_{\perp}$ with the concentration of TBATPB in other liquid crystals.[5,16] Thus, although the solubility of TBATPB decreases steadily from mixture A to F and thereby increases their resistivities, we believe that the $\sigma_{\parallel}/\sigma_{\perp}$ values of the different mixtures can be compared with one another. The general trend at room temperature is that the $\sigma_{\parallel}/\sigma_{\perp}$ value decreases as the molecular length of the mixture increases. As the temperature is increased, samples A–D show decreased $\sigma_{\parallel}/\sigma_{\perp}$ values, as expected in nematic LCs because of the decreasing order parameter. However, in mixtures E and F, the $\sigma_{\parallel}/\sigma_{\perp}$ values go through a maximum between 20 and 50° C. This general type of behavior in other nematics has been reported[17–19] to be due to cybotactic nematic[20] characteristics (i.e., short range smectic order in a nematic LC). In our phenyl benzoate mixtures, this is observed when the average length is 25.9 Å and longer, corresponding to an average of about 10 or more carbons from the combination of both alkyl end groups in the molecules (see Table III). It is interesting that none of the pure components in these mixtures is reported to be a smectic and that our DSC analysis also does not show any smectic phase in the components or their mixtures.

Because $\sigma_{\parallel}/\sigma_{\perp}$ is an anisotropic ratio that depends on the order parameter, we show in Figure 6 comparisons of the mixtures at two values of reduced temperature. For these mixtures, the lower temperature of $T = 0.91\ T_c$ is near 25° C, while the higher temperature of $T = 0.96\ T_c$ is near 42° C. At both temperatures, the $\sigma_{\parallel}/\sigma_{\perp}$ values decrease approximately linearly as the $\bar{L}$'s of the mixtures increase. This may be due to several factors. At the lower temperature, the increasing cybotatic nematic character with increasing $\bar{L}$ appears to be important. However, since similar effects are observed at 42° C, where the cybotatic effects should be less significant, other factors are probably involved. Qualitatively, we ascribe these other factors to the increasing percentage of the relatively flexible alkyl end groups compared to the more

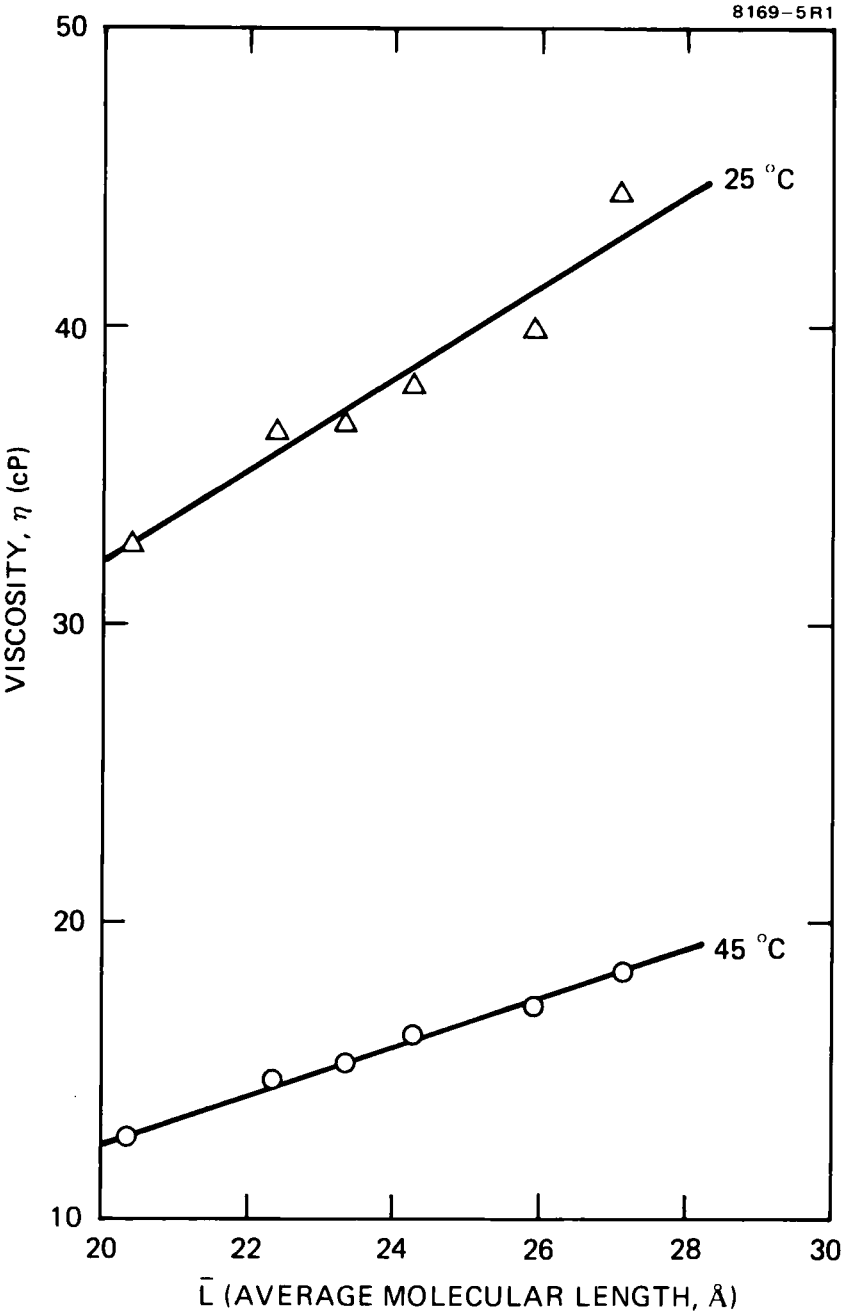

FIGURE 4 Flow viscosity of RO-R′ ester mixtures A-F as a function of their $\bar{L}$.

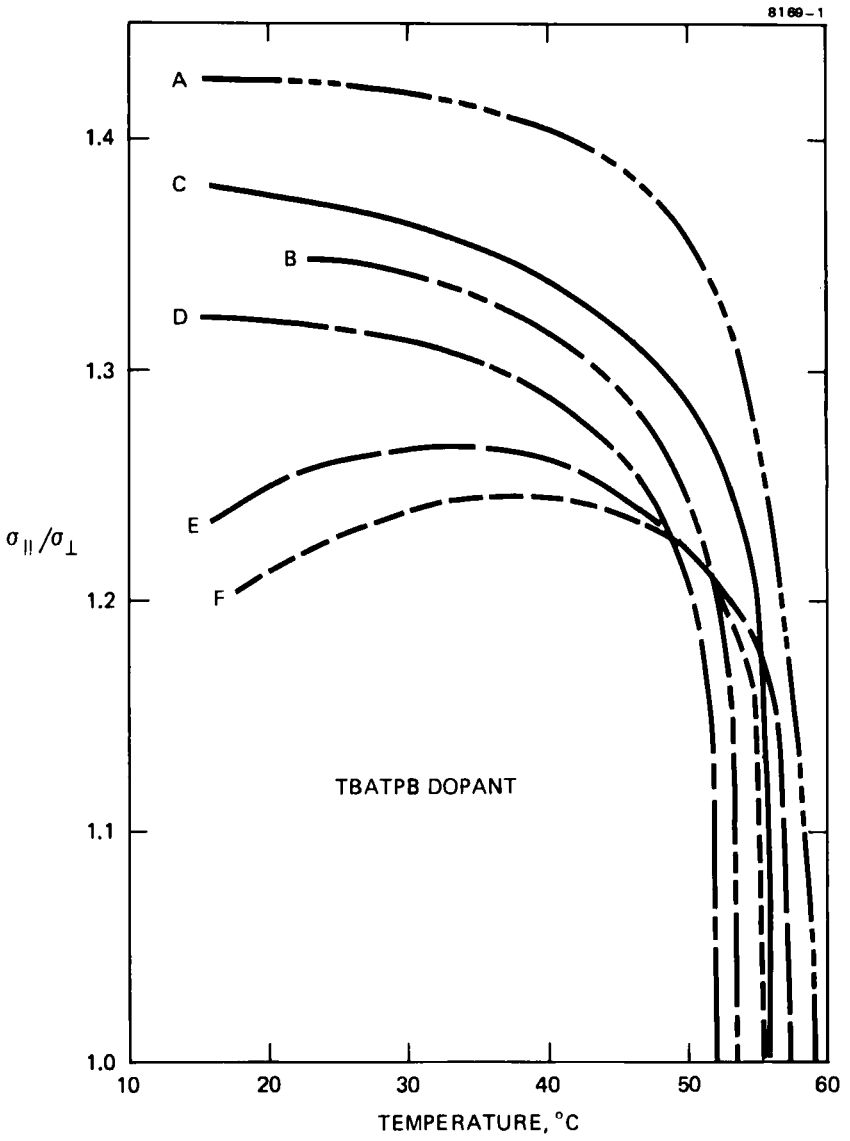

FIGURE 5 Conductivity anisotropy of TBATPB in RO–R′ ester mixtures as a function of temperature.

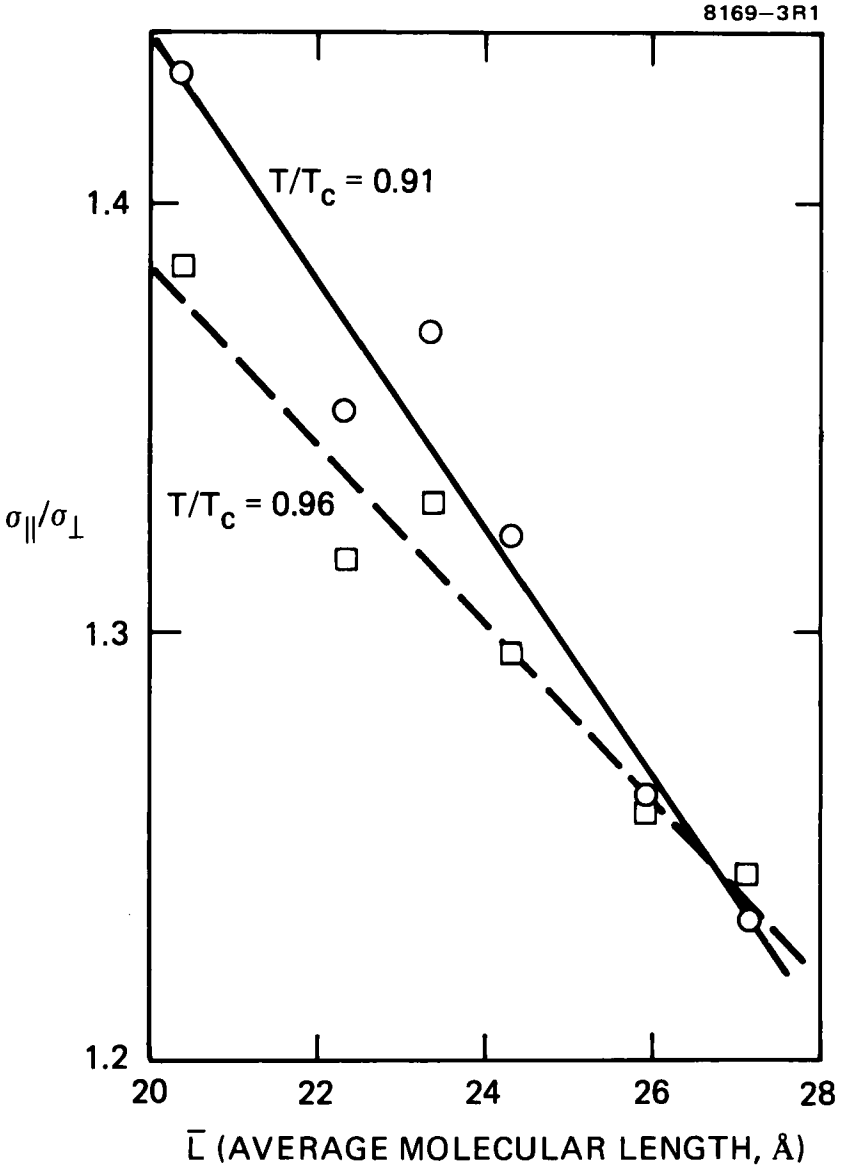

FIGURE 6 Effect of $\bar{L}$ of mixtures on their conductivity anisotropy at two reduced temperatures.

rigid central phenyl benzoate structure. The percentage of alkyl group length goes from 31.5% in mixture A up to 48.6% in mixture F. The transverse nematic flow viscosities (η_1 and η_3) probably do not increase as rapidly with $\bar{L}$ as η_2 does. Similarly, the $\sigma_\perp$ values probably do not decrease as rapidly with $\bar{L}$ as does $\sigma_\parallel$, thus causing a decrease in $\sigma_\parallel/\sigma_\perp$.

Dielectric anisotropy

The effects of temperature on the dielectric constants and dielectric anisotropy are shown for each mixture in Figures 7 and 8. The values of $\epsilon_\perp$ decrease almost linearly with increasing temperature. On the expanded scale used in Figure 8, it can be seen that, although small in magnitude, the $-\Delta\epsilon$ values in each mixture go through a maximum in the 35 to 40° C range. This is most pronounced with the shorter mixtures. In addition, at a given reduced temperature, the $\Delta\epsilon$ values become more negative as the average molecular length increases, as shown by the approximately linear plots in Figure 9. Both the temperature effect and the molecular length effect on $\Delta\epsilon$ are unexpected. We can only speculate that there is some type of weak intermolecular interaction that causes $\Delta\epsilon$ to be less negative in the shorter mixtures, and that this interaction decreases as the samples are heated. Such a molecular interaction might also decrease as the cybotatic nematic packing increases in the longer mixtures.

Field effect transition and elastic constants

The threshold voltage for the dielectric field-effect realignment (no conductive dopant) of the LC mixtures in surface-⊥ cells is shown in Figure 10, from optical birefringence measurements. This threshold voltage decreases with increasing $\bar{L}$ of the mixtures. The effect of $\bar{L}$ on the values of the bend elastic constant k_{33} are also shown in Figure 10, as calculated from the expression:

$$(V'_{th})_{FE} = \pi\left(\frac{k_{33}}{\epsilon_0|\Delta\epsilon|}\right)^{1/2}.$$

Dynamic scattering

The threshold voltage (V_{th}) for DS for the TBATPB-doped mixtures increases sharply with increasing average molecular length, as shown in Figure 11. This effect appears to be due primarily to the $\sigma_\parallel/\sigma_\perp$ values of these mixtures, as indicated by our observation that a Helfrich-type plot of V_{th}^{-2} versus $(\sigma_\parallel/\sigma_\perp)^{-1}$ is approximately linear, although such a linear relationship should actually be applicable only if all of the LC properties except $\sigma_\parallel/\sigma_\perp$ are constant.[5] Since we have found that k_{33}, ϵ, $\Delta\epsilon$, and η all vary with $\bar{L}$, this observation indicates that the $\sigma_\parallel/\sigma_\perp$ values probably have a dominant effect on V_{th} when comparing these mixtures at room temperature in surface-|| cells.

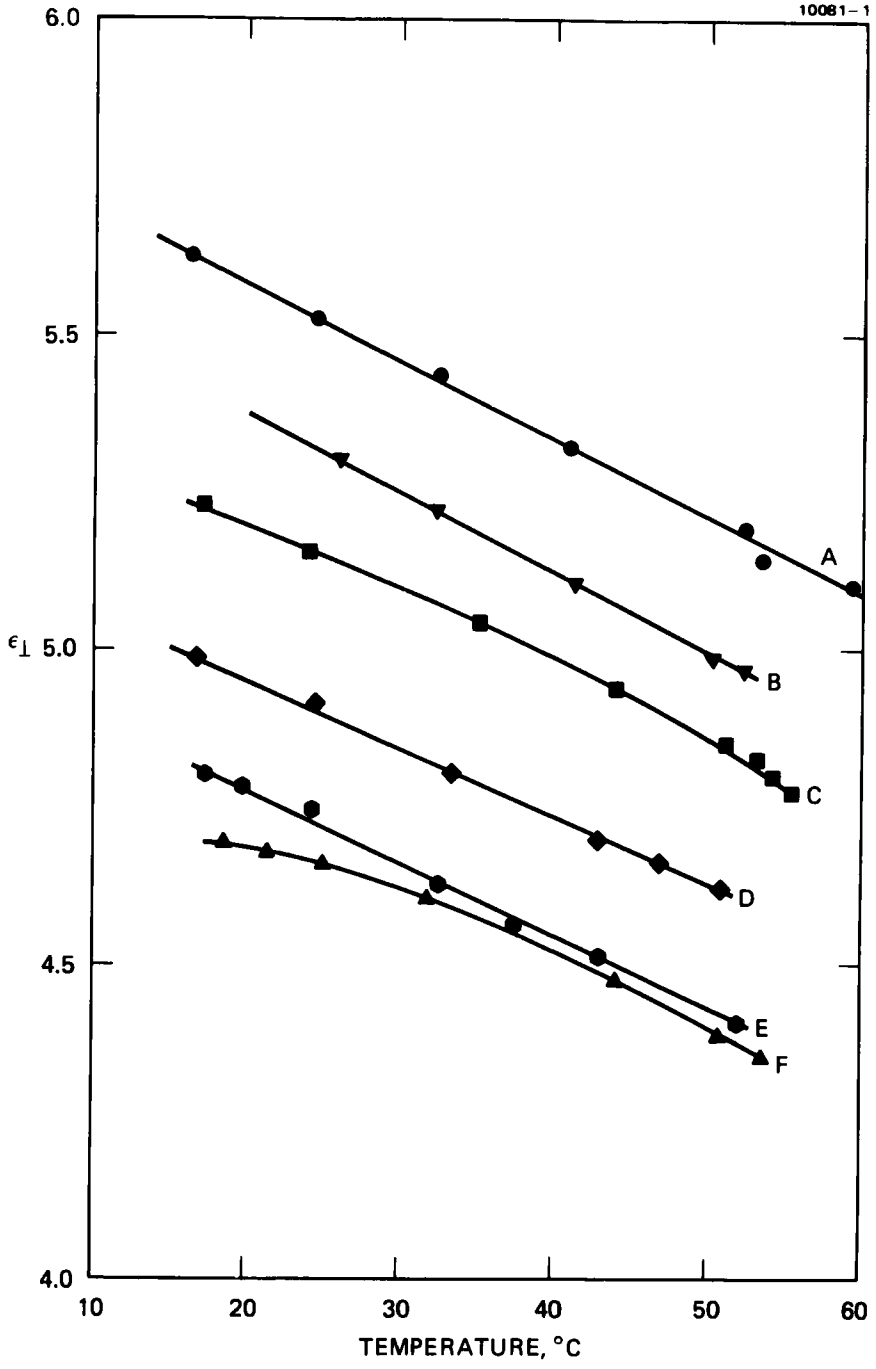

FIGURE 7 Dielectric constant ($\epsilon_\perp$) of RO-R′ mixtures as a function of temperature.

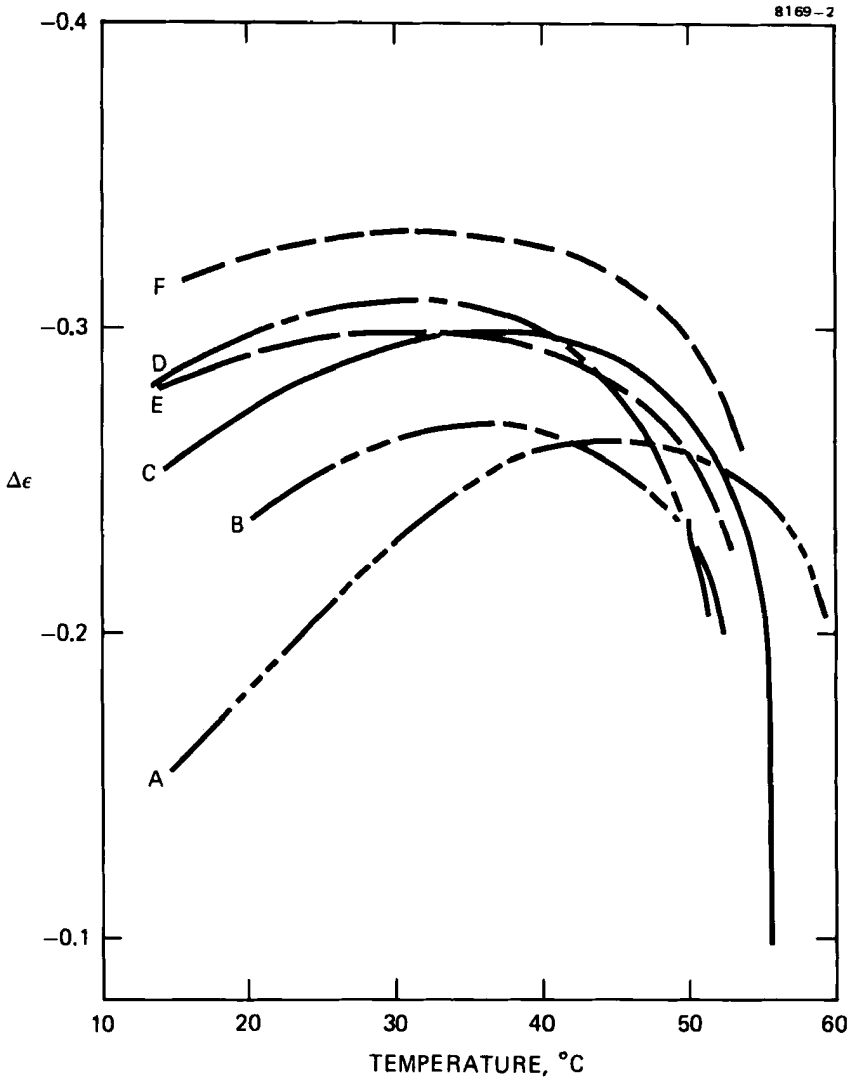

FIGURE 8 Dielectric anisotropy of RO-R′ mixtures as a function of temperature.

The results of our DS decay time studies at 25°C are shown in Figure 12. For comparison, the decay times are all corrected to a nominal cell thickness of 16.0 μm, using a factor of $16^2/l^2$. (As indicated in the experimental section, the actual thicknesses, l, of the surface-$\parallel$ cells are 15.86 and 15.43 μm, while for the surface-$\perp$ cell it is 15.90 μm.) The activated voltages used are high

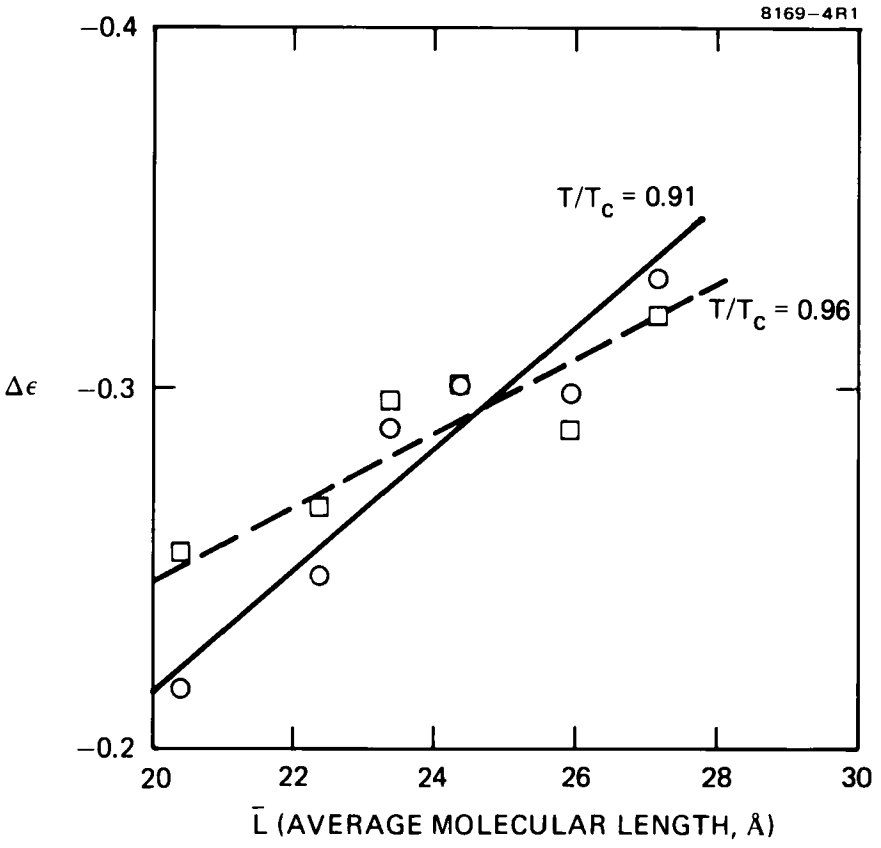

FIGURE 9 Effect of $\bar{L}$ of mixtures A-F on their dielectric anisotropy at two reduced temperatures.

enough to give at least 90% scattering in our optical system without causing secondary scattering. The decay times are all compared from the same relative transmission changes of 10%T to 90%T. The effect of $\bar{L}$ on the decay time is strikingly dependent on the initial LC surface alignment. The τ_D of the LC cells with surface-|| LC alignment decreases slightly with increasing L (even though the flow viscosity increases appreciably), and it is independent of the alignment method. On the other hand, the τ_D of the surface-$\perp$ cells increases with $\bar{L}$ even more rapidly than the increase in the LC flow viscosity with $\bar{L}$. As shown in Figure 12, the ratio $(\tau_D)_\perp/(\tau_D)_\parallel$ goes from about 1.5 at short $\bar{L}$ up to about 2.5 at long $\bar{L}$ values.

The decay time of DS cells has been reported to be directly proportional to viscosity[2] and to fit the equation: $\tau_D = C\eta l^2/k$, where C is a constant charac-

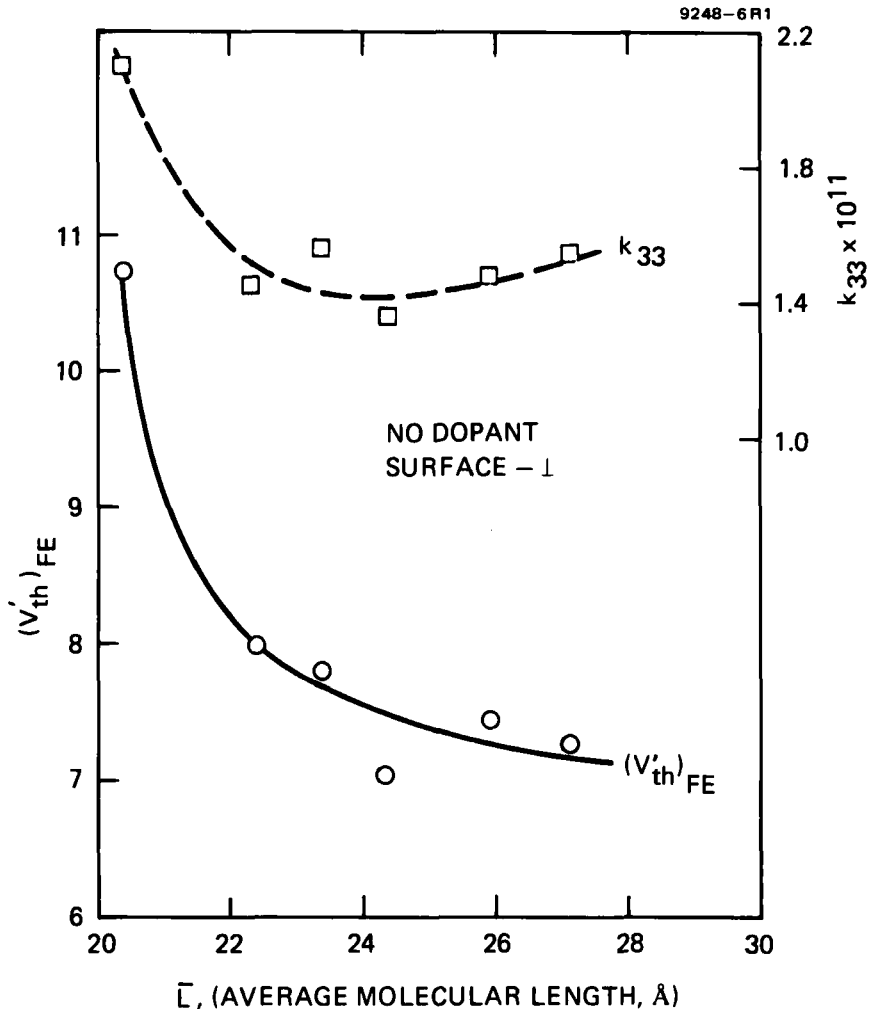

FIGURE 10 Effect of $\bar{L}$ of RO–R′ mixture on the dielectric field effect transition and k_{33} at 25°C. (The k_{33} unit is Newtons.)

teristic of the LC, η is the viscosity, and k is an elastic constant.[1] Similarly, the decay time for Williams domains has been expressed[21] by $\tau_D' = l^2\eta'/4\pi^2 k$, where η' is a "viscosity parameter and k is the appropriate elastic constant." In our series of mixtures at 25°C, $(\tau_D)_{\parallel}$ is nearly independent of η, while $(\tau_D)_{\perp}$ is directly proportional to η (where our $\eta \simeq \eta_2$). On the other hand, the variation of the ratio η_2/k_{33} with $\bar{L}$ is not directly proportional to the change of either $(\tau_D)_{\parallel}$ or $(\tau_D)_{\perp}$ with the $\bar{L}$ of these mixtures.

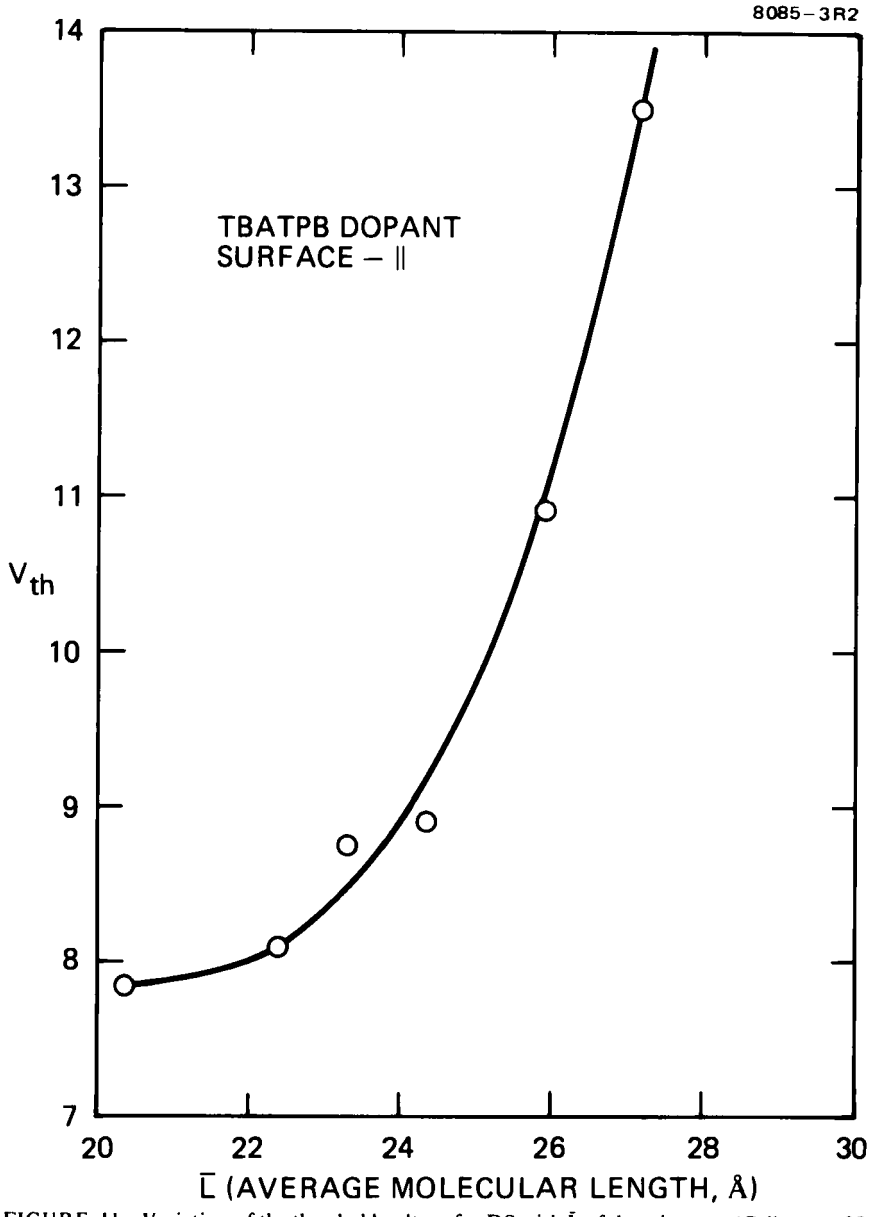

FIGURE 11 Variation of the threshold voltage for DS with $\bar{L}$ of the mixtures. (Cells are ~25 μm thick and have surface-|| alignment.)

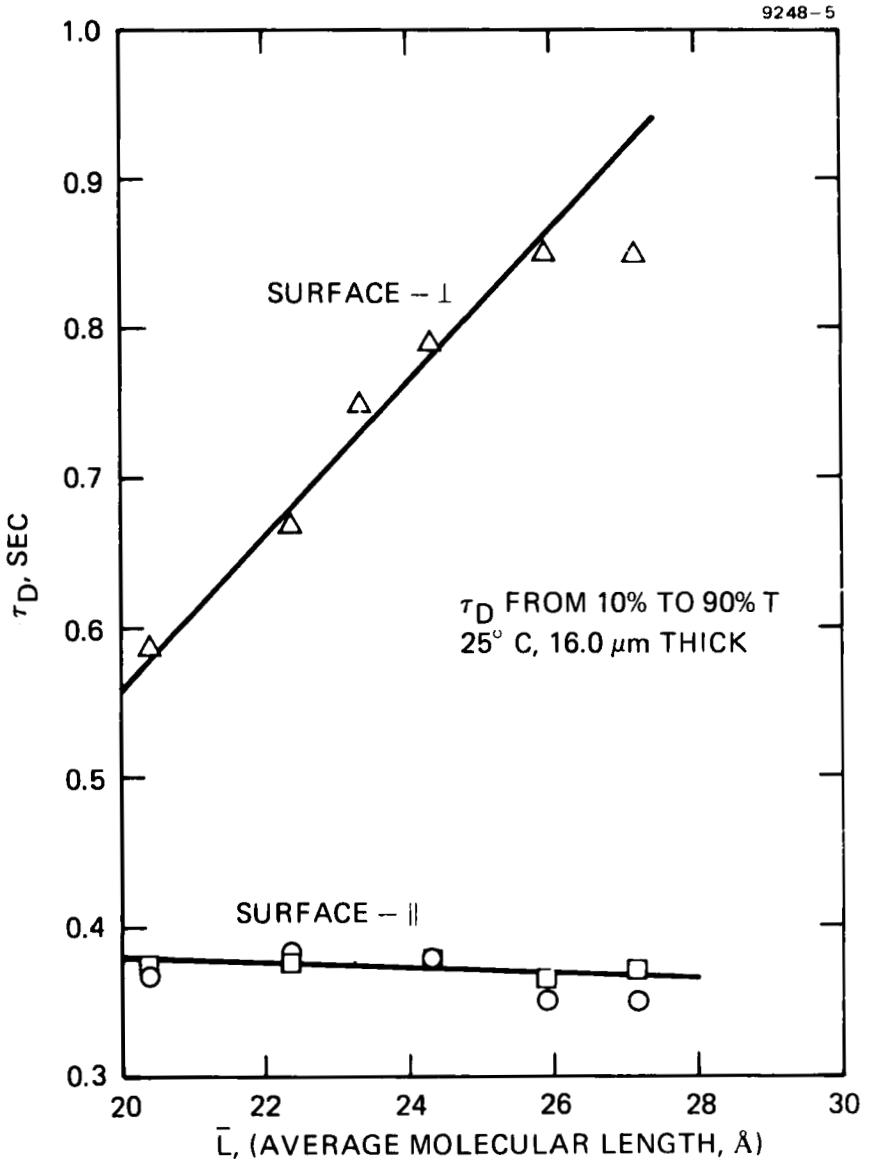

FIGURE 12 Effect of $\bar{L}$ on DS decay times. Surface-|| cells: ○—ion beam etched SiO_2, □—rubbed PVA; surface-⊥ cells: △—C_{18} alcohol treated SiO_2.

CONCLUSIONS

Comparisons of *p*-alkoxyphenyl *p*-alkylbenzoate nematic mixtures with similar clearpoints show that several of their properties vary linearly with the average molecular length of the mixtures: the flow viscosity increases with $\bar{L}$, while the refractive index, birefringence, density, conductivity anisotropy, dielectric constants, and dielectric anisotropy decrease as $\bar{L}$ increases. The temperature dependence of $\sigma_{\parallel}/\sigma_{\perp}$ shows that mixtures with a total average of more than 10 carbon atoms from both aliphatic end groups have cybotactic nematic characteristics. The shorter length mixtures are advantageous for DS applications primarily because they have higher $\sigma_{\parallel}/\sigma_{\perp}$ values, lower threshold values for DS, and better solubility of conductive dopants than in the longer $\bar{L}$ mixtures. In surface-$\parallel$ cells, $\bar{L}$ has very little effect on the DS decay time at 25°C; however, in surface-$\perp$ cells, the decay time increases steeply (linearly) with $\bar{L}$. Thus, in surface-$\perp$ cells, the shorter $\bar{L}$ mixtures are advantageous for faster decay times.

Acknowledgments

We are indebted to the Directorate of Chemical Sciences, Air Force Office of Scientific Research, Contract F49620-77-C-0017, for partial financial support of this research; to S.-M. Wong and C. I. van Ast for assistance in synthesis; and to W. H. Smith, Jr., for assistance in the DSC measurements.

References

1. L. T. Creagh, *Proc. IEEE,* **61,** 814 (1973).
2. U. Bonne and J. P. Cummings, *IEEE Trans. Elec. Devices,* **ED-20,** 962 (1973).
3. H. S. Lim and J. D. Margerum, *Appl. Phys. Lett.,* **28,** 478 (1976).
4. J. D. Margerum and L. J. Miller, *J. Colloid and Interface Sci.,* **58,** 559 (1977).
5. J. D. Margerum, H. S. Lim, P. O. Braatz and A. M. Lackner, *Mol. Cryst. Liq. Cryst.,* **38,** 219 (1977).
6. H. S. Lim, J. D. Margerum and A. Graube, *J. Electrochem. Soc.,* **124,** 1389 (1977).
7. E. C-H. Hsu and J. F. Johnson, *Mol. Cryst. Liq. Cryst.,* **20,** 177 (1973).
8. D. Demus, C. Fietkau, R. Schubert and H. Kehlen, *Mol. Cryst. Liq. Cryst.,* **25,** 215 (1974).
9. M. J. Little, H. L. Garvin and L. J. Miller, *Liquid Crystals and Ordered Fluids,* **3,** p. 497, J. E. Johnson and R. S. Porter, eds. (Plenum Press, 1978).
10. L. J. Miller, J. Grinberg, G. D. Myer, D. S. Smythe and W. H. Smith, *Liquid Crystals and Ordered Fluids,* **3,** p. 513, J. E. Johnson and R. S. Porter, eds., (Plenum Press, 1978).
11. D. Meyerhofer, *J. Appl. Phys.,* **46,** 5084 (1975).
12. B. H. Soffer *et al., Proc. SPIE,* **81,** 218 (1980).
13. B. H. Soffer, J. D. Margerum, A. M. Lackner, *et al., Mol. Cryst. Liq. Cryst.* (in press). July 1980. *Mol. Cryst. Liq. Cryst.* (in press).
14. M. E. Neubert, L. T. Carlino, R. D'Sidocky and D. L. Fishel, *Liq. Cryst. and Ordered Fluids,* (Plenum Press, New York, 1974), **2,** p. 293, J. Johnson and Porter, eds.
15. A. E. White, B. E. Cladis and S. Torza, *Mol. Cryst. Liq. Cryst.,* **43,** 13 (1977).
16. J. D. Margerum, A. M. Lackner and H. S. Lim, Paper DP28, 7th International Liq. Cryst. Conf., Bordeaux, France, 1978.
17. F. Rondelez, *Solid State Comm.,* **11,** 1675 (1972).

18. A. Mircea-Roussel, L. Legar, F. Rondelez and W. H. DeJeu, *J. de Physique, Colloq.*, **C136,** 93 (1975).
19. G. Heppke and F. Schenider, *Z. Naturforsch,* **309,** 316 (1975).
20. A. DeVries, *J. de Physique (Paris) Colloq.*, **C136,** 1 (1975).
21. G. Meier, E. Sackman and J. G. Grabmaier, *Application of Liquid Crystals,* (Springer Verlag, Berlin, 1975), p. 16.